

Structure of the SMC

Stellar component distribution from 2MASS data

I. Gonidakis¹, E. Livanou¹, E. Kontizas², U. Klein³, M. Kontizas¹, M. Belcheva¹, P. Tsalmantza⁴, and A. Karamelas¹

¹ Department of Astrophysics Astronomy & Mechanics, Faculty of Physics, University of Athens, GR-15783 Athens, Greece

² Institute for Astronomy and Astrophysics, National Observatory of Athens, P.O. Box 20048, GR-11810 Athens, Greece

³ Radioastronomisches Institut der Universität Bonn, Auf dem Hugel 71, D-53121 Bonn, Germany

⁴ Max-Planck-Institut für Astronomie, Königstuhl 17, 69117 Heidelberg, Germany

Received date / accepted

ABSTRACT

Aims. The spatial distribution of the SMC stellar component is investigated from 2MASS data. The morphology of the different age populations is presented. The center of the distribution is calculated and compared with previous estimations. The rotation of the stellar content and possible consequence of dark matter presence are discussed.

Methods. The different stellar populations are identified through a CMD diagram of the 2MASS data. Isoleth contour maps are produced in every case, to reveal the spatial distribution. The derived density profiles are discussed.

Results. The older stellar population follows an exponential profile at projected diameters of about 5 kpc ($\sim 5^\circ$) for the major axis and ~ 4 kpc for the minor axis, centred at RA: $0^h 51^{min}$, Dec: $-73^\circ 7'$ (J2000.0). The centre coordinates are found the same for all the different age population maps and are in good accordance with the kinematical centre of the SMC. However they are found considerably different from the coordinates of the centre of the gas distribution. The fact that the older population found on an exponential disk, gives evidence that the stellar content is rotating, with a possible consequence of dark matter presence. The strong interactions between the MCs and the MilkyWay might explain the difference in the distributions of the stellar and gas components. The lack in the observed velocity element, that implies absence of rotation, and contradicts with the consequences of exponential profile of the stellar component, may also be a result of the gravitational interactions.

Key words. SMC – structure – dark matter

1. Introduction

SMC is classified as an irregular dwarf galaxy, characterized by a pronounced central feature of a Bar and an eastern extension called the Wing. There has been a lot of investigation carried out studying the distribution of different stellar populations of this galaxy. Initially, Freeman (1970) has calculated the scale length of the exponential component of the SMC from B-magnitude photometry. He has found $a^{-1}=0.63$ kpc. A long time later, Gardiner & Hawkins (1991) have found for a northern direction an exponential profile with $a^{-1}=1.2$ kpc, describing well the distribution up to $r=6$ kpc. However this value was calculated over the observed projected radial distribution assuming a spherically symmetric halo structure.

Morgan & Hatzidimitriou (1995) have carried out a spectroscopic survey of carbon stars in the outer parts of the SMC. Regarding the spatial distribution of these stars, they conclude that at most surface densities the SMC appears elliptical with major axis parallel to the Bar, but there is a significant northward distortion of the outer contours. The diameter of the outermost contour is $\sim 10^\circ$ - 12° . The authors also underline the existence of a spiral-arm-like extension of the carbon stars distribution southwards at (projected) distances larger than 4° (~ 4 kpc) from the optical centre, although its origin is not clear.

Counts of sources towards the Magellanic Clouds from DENIS near-infrared survey have been studied by Cioni et al.

(2000). Their investigation was based on the differentiation in the (I-J, I) Colour Magnitude Diagram (CMD) in order to distinguish between three groups of objects with different mean ages. The spatial distribution of the three age groups is found quite different the youngest stars exhibit an irregular structure while the older stars are smoothly and regularly distributed. The AGB and RGB stars are characterised by a regular, but double peaked, structure, an offset from the HI distribution, and a mean age difference of the two maxima.

Maragoudaki et al. (2001) have studied the spatial distribution of the SMC stellar population according to their age, based on optical data. They have shown that the older stellar population shows a rather regular and smooth distribution, while the youngest stellar component (age less than 8×10^6 yr) appears mainly along the northeast-southwest direction forming the Bar.

Stanimirovic et al. (2004) in a detailed study of the HI kinematics conclude that the HI velocity field shows a large velocity gradient from the south west to the north east. The isovelocity contours of this velocity field show some symmetry, suggestive of a differential rotation. Some large-scale distortions in this velocity field are easily visible but could be related to positions of several supergiant shells. In the same article the authors conclude that, in contrast to HI distribution the old stellar populations appear to have a spheroidal spatial distribution and a total absence of rotation.

In order to further investigate this discrepancy between the gas and stellar component distribution, we have studied the distribution of the various stellar components of the SMC from near

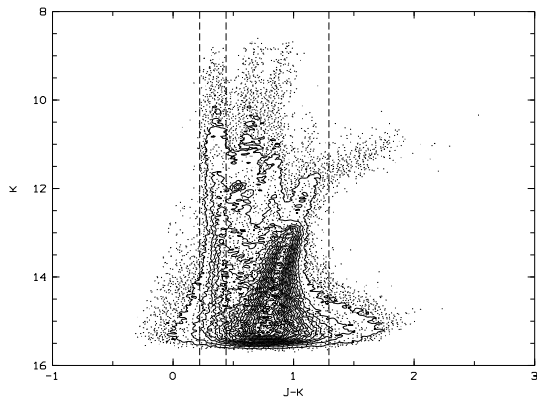


Fig. 1. Colour Magnitude Diagram K vs. J-K, of the SMC, from 2MASS

IR surveys. We know that IR observations characterize the mass of the galaxy better than those in shorter wavelengths where absorption masks a large part of the stellar component. A detailed study of the stellar component as it is revealed from 2MASS is given in section 2. A comparison with available radio data is given in section 3, implementing the same approach used for the near IR data. Discussion and conclusions are given in section 4.

2. 2MASS data

The near-infrared (NIR) images were obtained by the Two-Micron All-Sky Survey (2MASS), an ongoing effort to map the entire sky at J-band (1.25 microns), H-band (1.65 microns) and K-band (2.17 microns) wavelengths. The 2MASS survey is led by the University of Massachusetts, with all data and images processed at Caltech's Infrared Processing and Analysis Centre (IPAC). The survey utilizes two nearly identical 1.3-meter telescopes located at Mount Hopkins (Arizona) and at Cerro Tololo (Chile). While the pixel size is 2.0 arcseconds, the survey strategy of over-sampling yields an effective resolution of about 1 arcsecond. Exposure times are 7.8 seconds. 2MASS has uniformly scanned the entire sky in three near-infrared bands to detect and characterize point sources brighter than about 1 mJy in each band, with signal-to-noise ratio (SNR) greater than 10. This has achieved an 80,000-fold improvement in sensitivity relative to earlier surveys. The data used here are from the 2MASS All-Sky Point Source Catalog (PSC) (fp_psc), at IPAC Infrared Science Archive (IRSA), Caltech/JPL (<http://irsa.ipac.caltech.edu/applications/Gator>).

IRSA gives choices for the origin of the default magnitudes and uncertainties in each band. We have requested only sources with satisfying quality of photometry for all J, H and K band. In order to accomplish that we choose the case where: the default magnitude is derived from a profile-fitting measurement made on the 1.3 sec "Read_2" exposures. The profile-fit magnitudes are normalized to curve-of-growth-corrected aperture magnitudes. This is the most common type in the PSC, and is used for sources that have no saturated pixels in any of the 1.3 sec exposures.

The examined area of SMC is $6.9^\circ \times 12^\circ$. Data from a small near by field of $2.1^\circ \times 1^\circ$ are also obtained in order to be used later on for calculating the Galactic contribution. The coordinates of this near by field are $47.5 \leq \text{R.A.} \leq 60$ and $-68 \leq \text{Dec.} \leq -67$. It was selected to be close, but out of the SMC field, in order to represent well the distribution of

background stars near SMC. The dimensions were chosen to be big enough to make statistics for the SMC field. The initial catalogues contain 359234 stars for the SMC area and 10444 stars for the small nearby field. Total photometric uncertainty for 2MASS data is given by IRSA (details at http://www.ipac.caltech.edu/2mass/releases/allsky/doc/sec4_5e.html). Sources with total photometric uncertainty greater or equal to 0.2 mag for any of the J, H and K bands were excluded, providing more reliable photometric measurements. Finally the catalogues used contain 293330 stars for the SMC field and 8428 stars for the small nearby field.

2.1. Identifying Stellar populations

Major stellar populations are identified based on matching features of the observed colour-magnitude diagram with expected positions of known populations. Based on Hiparchos data of SMC stars, Gavras (2003) has determined the criteria for the different star types on the K versus J-K CMD of the SMC. The A, B type stars are found at $-1 < \text{J-K} \leq 0.2$ and $\text{K} \leq 15$. The F and G type have $0.2 < \text{J-K} \leq 0.45$ and $\text{K} \leq 15$. The K, M and faint Carbon Stars meet the criteria of $0.45 \leq \text{J-K} \leq 1.3$ and $\text{K} \leq 15$ and finally Carbon stars have $\text{J-K} \geq 1.3$ and $\text{K} \leq 15$. Applying the criteria above, to the 293330 stars for the SMC field we find 2618 A, B type stars, 30042 of F and G type, 177471 K, M and faint Carbon Stars and 4705 Carbon stars.

Two CMDs: the K vs J-K for the SMC area and the nearby field were produced. Both diagrams are divided in a grid with the same number of cells (22×16). The cells have dimensions that provide a fine grid, while they include enough number of stars to make statistics. The grids had the same number of cells and same starting and ending points for each axis, in order to compare numbers of stars with same K and J-K values. The cells of the nearby field were normalized to the equal area of the cells of the SMC area and their stars considered as background stars were subtracted randomly. The CMD of K versus J-K for the SMC field after subtraction of the background contribution is shown in Fig.1. The criteria set by Gavras (2003) for J-K values are indicated by the dashed lines.

Since the different populations were defined, star counts were performed in a grid of 288×500 pixels for the SMC region. The isopleths contour maps of the SMC field that were produced for each of the four cases can be seen in Fig.2. It is very interesting to point out how well the old population (bottom right in Fig.2) reveals the center of mass of this stellar population.

2.2. Distribution of late type stars

In the case of K, M and faint Carbon stars the distribution reveals the elliptical structure of a disk. The number density of the stars versus the distance from the centre has been estimated. The isopleths contour map of the SMC field was reproduced (Fig.3) with bigger steps between the contours in order to allow more accurate selection of the image points that will be taken under consideration. The outermost contour is the same as in Fig.2 and will be the one specifying the diameter of each structure. We selected 4 directions a, b, c and d along the "minor" and "major" axis to derive their density profiles. The "major" axis is the one following the direction of the Bar, from north-east to south-west, while the "minor" axis is directing from south-east to north-west.

Fitting exponential curves to the diagrams of number density of sources (N) versus (projected) distance from the centre of the galaxy (r), with exponential functions was

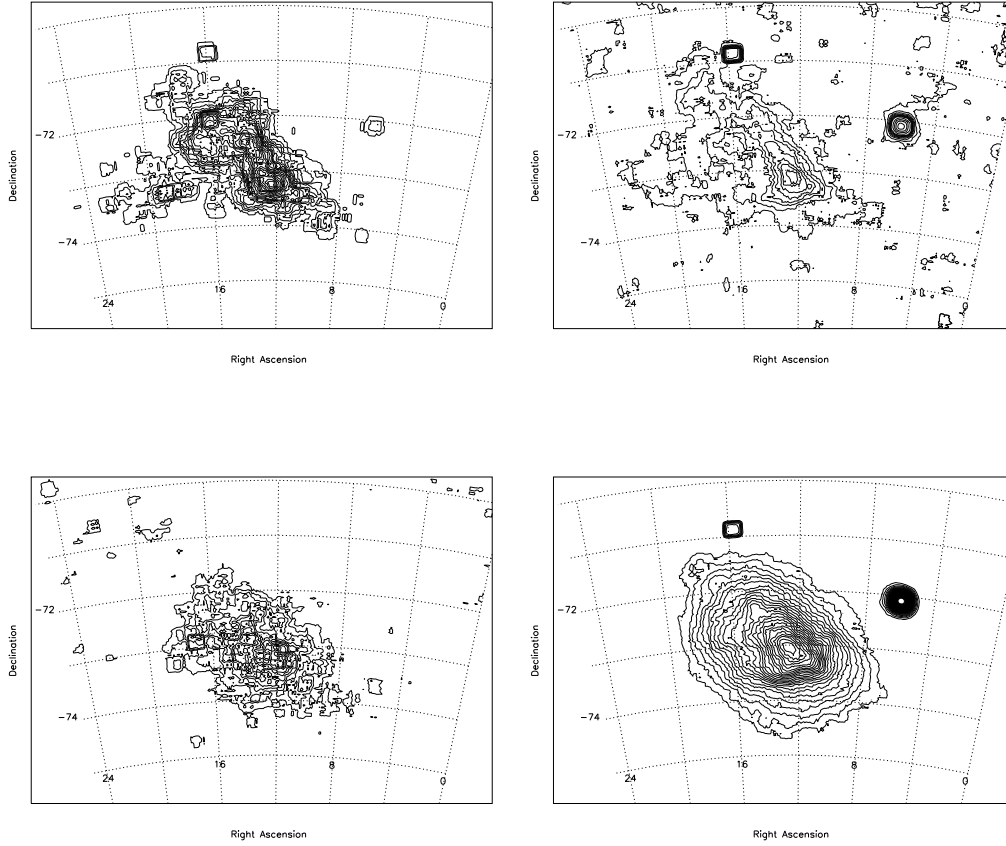


Fig. 2. Isopleths contour maps of the SMC different stellar populations, from 2MASS. Top left: A and B type stars, top right: F and G, bottom left: Carbon stars and bottom right: K, M and faint Carbon.

very satisfying. The best fit functions are $Y=15.9\pm 2.2*\exp(-1.0\pm 0.5*X)-0.8\pm 3.1$, $Y=19.7\pm 6.8*\exp(-0.4\pm 0.3*X)-4.7\pm 8.1$, $Y=16.6\pm 1.8*\exp(-1.5\pm 0.6*X)+0.3\pm 2.0$, $Y=17.8\pm 2.0*\exp(-1.3\pm 0.5*X)-0.1\pm 2.1$, for the directions a, b, c and d respectively. The values of a^{-1} are 1.0, 2.5, 0.7 and 0.8 derived for each direction respectively, corresponding to a mean value of $a^{-1}=1.25$ kpc. For the power-law scenario, the best fit functions are $Y=5.0\pm 0.5*X^{(-0.6\pm 0.1)}$, $Y=6.8\pm 0.5*X^{(-0.6\pm 0.1)}$, $Y=4.2\pm 0.6*X^{(-0.8\pm 0.1)}$, $Y=5.0\pm 0.5*X^{(-0.8\pm 0.1)}$, for the directions a, b, c and d respectively. The chi-square parameters are 0.04, 0.03, 0.09 and 0.11 in the case of exponential fitting curves for the directions a, b, c and d respectively. The corresponding values for the power-law case are 1.6, 2.4, 1.0 and 2.4, indicating that exponential fitting represents better the data. Consequently the mass distribution derived here is described by an exponential disk as illustrated in Fig. 4 with the best fitting curves. Summing up, 2MASS reveals an exponential profile for the older stellar population with a (projected) diameter ~ 3.8 kpc for the "minor" axis and ~ 4.8 kpc for the "major" axis. The center of the elliptical distribution is best determined by the right bottom map of Fig. 2, at RA: $0^h 51^m$, Dec: $-73^\circ 7'.2$, that represents the K, M and faint carbon stars.

The exponential disk model for K, M and faint Carbon stars, has to face the fact that the values of a^{-1} are not found the same for the semi-axis's, and the fact that exponential along direction (d) is measured to be "steeper" than the exponential along direction (a). The observed asymmetry might be explained by the

inclination of the SMC, although deprojection procedure is not clear enough in the case of this galaxy. However further investigation should put light on this issue.

3. Radio data

A radio image of SMC at 1400 GHz (21cm) was obtained from Uli Klein (private communication) based on the data that were derived from the work by Haynes et al. (1986). The data represent well the extended radio envelope of the SMC, well beyond any site of obvious active star formation and are appropriate for investigating the gas distribution at the SMC. The radial profile of this image is presented in Fig. 5. Using the previous methodology we created diagrams of flux density (F) versus distance from the centre (r), and fitted data with exponential and power-law curves in order to reveal the most efficient mathematical description of this distribution. The best fit exponential functions we found are $Y=1208.1\pm 2.0*\exp(-2.2\pm 0.01*X)+30.7\pm 1.9$, $Y=17243.6\pm 270.6*\exp(-3.7\pm 0.02*X)+28.2\pm 2.1$, $Y=1801.9\pm 21.2*\exp(-1.33\pm 0.02*X)-585.6\pm 14.6$, and $Y=248641.0\pm 6690.8*\exp(-4.5\pm 0.02*X)+60.13\pm 1.6$, for the directions a, b, c and d respectively. The values of a^{-1} are 0.45, 0.27, 0.75 and 0.22 derived for each direction respectively, corresponding to a mean value of $a^{-1}=0.42$ kpc. For the power-law case, the best fit functions are $Y=241.6\pm 0.5*X^{(-0.8\pm 0.001)}$, $Y=456.9\pm 0.5*X^{(-3.4\pm 0.01)}$,

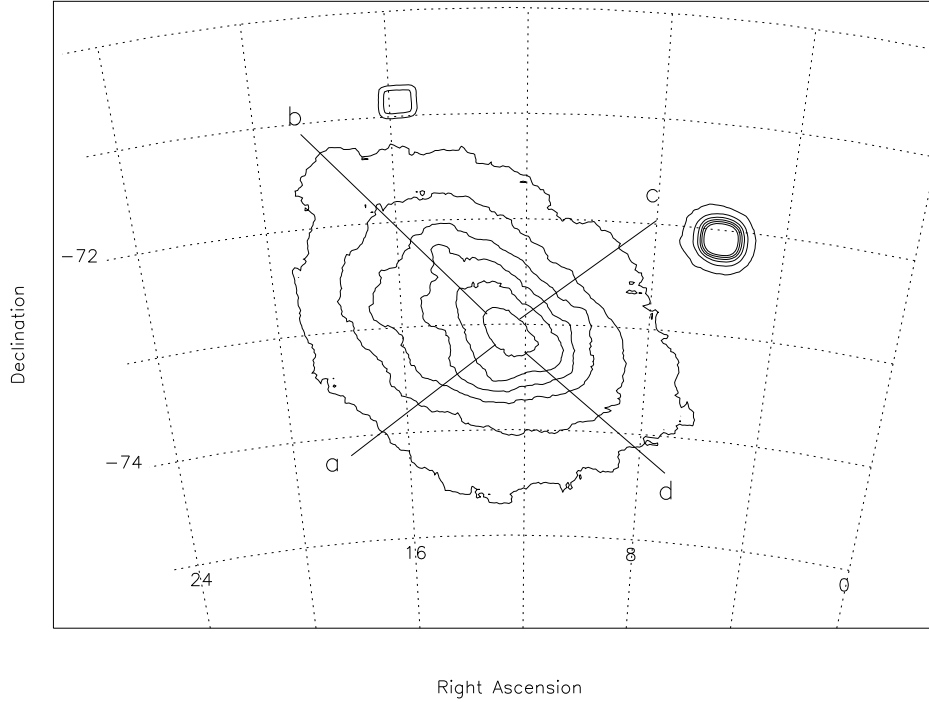


Fig. 3. Isopleths contour map of the SMC K, M and faint Carbon Stars, from 2MASS. Lines indicate the selected directions. The "major" axis of the galaxy is the one following the direction of the Bar, from north-east to south-west, while the "minor" axis is directing from south-east to north-west.

$Y=191.7\pm 0.5*X^{(-0.9\pm 0.002)}$, $Y=3087.4\pm 10.8*X^{(-5.5\pm 0.01)}$, for the directions a, b, c and d respectively. The chi-square parameters are 590.0, 390.8, 33.8 and 471.9 in the case of exponential fitting curves for the directions a, b, c and d respectively, whereas the corresponding values for the power-law case are 5542.13, 11285.9, 188.0 and 419.5. The comparison of the two sets of parameters allow us to suggest that exponential fitting represents better the distribution. We notice however, that in for direction (d) power-law is more efficient the Consequently the mass distribution derived here is described by an exponential disk as illustrated in Fig. 6 with the best fitting curves.

These led us to a mean value of $a^{-1} = 0.42$ kpc for the radio data. The centre is found at RA: $0^h 55^m 7^s.2$, Dec: $-72^\circ 47' 59''$. The HI exponential profile has a scale length of 0.45 kpc along the south-east direction (a), 0.27 kpc along the north-east direction (b), 0.75 kpc along the to north-west direction (c) and 0.22 kpc along the south-west direction (d). These coordinates of the center are in accordance with the results of Stanimirovic et al. (2004) derived from higher resolution data, and confirms that the differences found here between the central coordinates of the stellar and the gas component are real.

4. Discussion & Conclusions

The distribution of the stellar components in the near IR (2MASS) has been used to investigate the radial distribution of the stellar mass in the SMC. The isopleths in near IR wave-

lengths are expected to represent more accurately the distribution of stars since the observations are less affected by absorption.

In the case of the 2MASS data we set the criteria for collecting the different stellar populations and present their spatial distributions. It has been found that exponential profile fits better the distribution of the older population of the SMC. In Fig. 2 the bottom right map of K, M and faint carbon stars, reveals extremely accurately the center of the mass distribution of the oldest stellar population of the SMC, the coordinates of this center are found to be the same for all cases, independently the age of population they represent.

This centre of the isopleths is found to be RA: $0^h 51^{min}$, Dec: $-73^\circ 7'$ and the mean value for scale length is $a^{-1} = 1.25$ kpc.

4.1. The center offset

The important characteristic of the distribution of the older stellar population of the SMC is found to be the offset of the center of their distribution from the centre of the distribution found by HI data (Stanimirovic et al., 2004). In a more recent work, Piatek et al. (2007) have calculated the kinematical centre of the SMC at RA: $0^h 52^m.8$, Dec: $-72^\circ 30'$ from HST data being in good agreement with our calculations. They also explain that the presence of a Bar or a strong tidal disturbance can infer extra streaming motions to a system and thus old and young populations can have distinct kinematics. The strong interactions

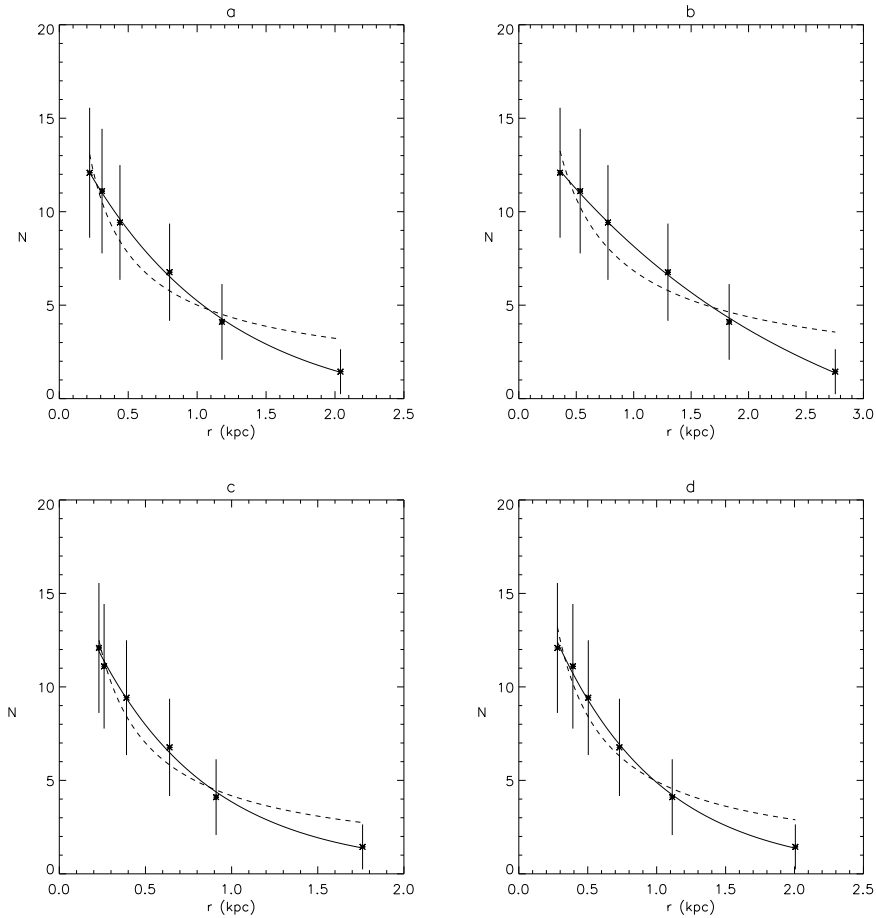


Fig. 4. Number of stars per pixel (N) vs. distance from the centre (r) (star symbols), fitted with exponential curves (solid lines) and power-law curves (dashed lines), for 2MASS data for the a, b, c and d directions respectively.

of the SMC with the LMC and the MilkyWay that have probably contributed to the formation of the Bar (Maragoudaki et al., 2001) could also have as a result the observed difference in the centres of the distributions of the stellar and the gas component as well as the small radial velocity gradient among SMC stars (Bekki & Chiba, 2008), that contradicts with the exponential profile of the stellar component.

Stanimirovic et al. (2004) suggest that according to SMCs rotation curve a dark matter halo is not needed to explain its dynamics. However reconsidering the values of the center of the SMC, adopting the center of the mass derived above, when calculating rotational velocity profiles may be important considering the issue of dark matter presence in this galaxy. SMC is a dwarf irregular galaxy, which are expected to be dark matter dominated (Cote et al. 2000; Begum et al. 2006; Strigari et al. 2008). However, rotational velocities do not support this case for SMC, probably because they have been affected by the interactions of the Magellanic system with the Milky way.

4.2. The scale length values

As mentioned before, Freeman (1970) has investigated the structure of the SMC through bright stars distribution and has found that their elliptical component is characterised by a scale length of $a^{-1}=0.63$ kpc. We find an exponential profile for the older stellar population with $a^{-1}=1.25$ kpc, while the gas exponential disk has $a^{-1}=0.42$ kpc. These three values represent well the

structure of three different galactic components and are in accordance with the fact that gas (radio data) is more concentrated on a thinner disk, younger stars (best represented by B-magnitude distribution) lay on a thicker disk and finally oldest stars reach bigger distances from the center.

5. Acknowledgements

The authors would like to thank the University of Athens (ELKE) for partial financial support. The project is co-funded by the European Social Fund and National Resources-(EPEAEK II) PYTHAGORAS II.

References

- Begum, A., Chengalur, J. N., Karachentsev, I. D., Kaisin, S. S., & Sharina, M. E. 2006, *MNRS*, 365, 1220
- Bekki, K., & Chiba, M. 2008, *astro-ph*, 0806.4657
- Cioni, M.-R. L., Habing, H. J., & Israel, F. P. 2000, *A&A*, 358, L9
- Cote, S., Carignan, C., & Freeman, K. C. 2000, *AJ*, 120, 3027
- Freeman, K. C. 1970, *ApJ*, 160, 811
- Gardiner, L. T., & Hawkins, M. R. S. 1991, *MNRAS*, 251, 174
- Gavras, P. 2003, MSc thesis University of Athens
- Haynes, R. F., Klein, U., Wielebinski, R., & Murray, J. D. 1986, *A&A*, 159, 22
- Maragoudaki, F., Kontizas, M., Morgan, D. H., et al. 2001, *A&A*, 379, 864
- Morgan, D. H., & Hatzidimitriou, D. 1995, *A&AS*, 113, 539
- Piatek, S., Pryor, C., & Olszewski, E. W. 2007, *astro-ph*, 0712.176
- Stanimirovic, S., Staveley-Smith, L., & Jones, P. A. 2004, *ApJ*, 604, 176
- Strigari, L. E., Koushiappas, S. M., Bullock, J. S., et al. 2008, *ApJ*, 678, 614

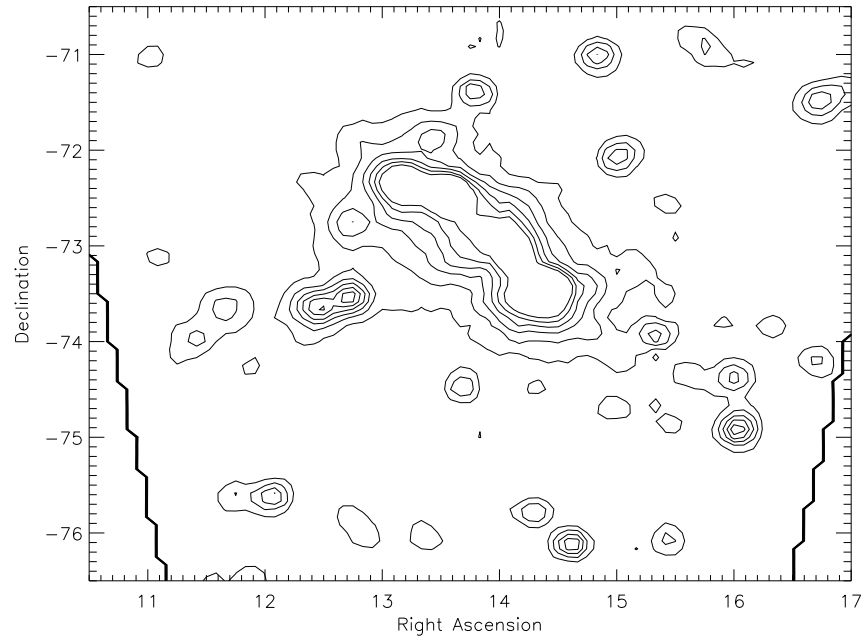


Fig. 5. Isodensity contour map of the SMC radio data.

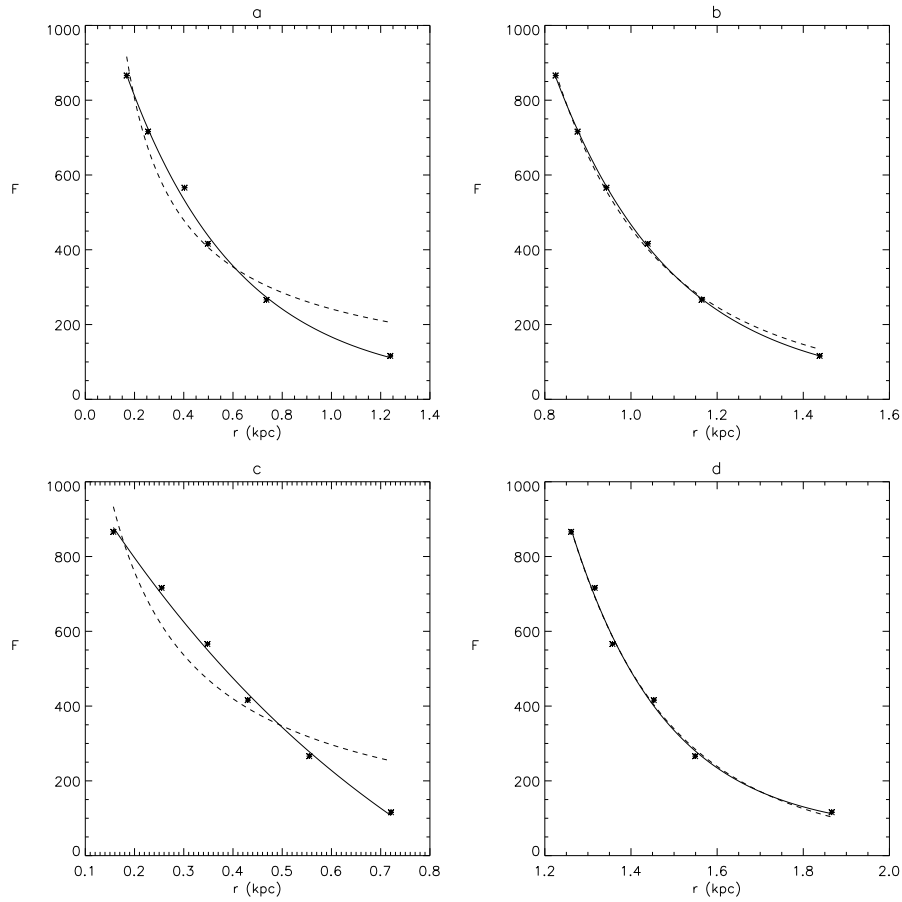


Fig. 6. Flux density (F) versus distance from the centre (r) (star symbols), fitted with exponential curves (solid lines) and power-law curves (dashed lines), for radio data for the a, b, c and d directions respectively.